RNA (2001), *7*:64–70. Cambridge University Press. Printed in the USA.

Functional mapping of ribosome-contact sites in the ribosome recycling factor: A structural view from a tRNA mimic

TOSHINOBU FUJIWARA, KOICHI ITO, and YOSHIKAZU NAKAMURA

Department of Basic Medical Sciences, The Institute of Medical Science, The University of Tokyo, Tokyo 108-8639, Japan

ABSTRACT

Ribosome recycling factor (RRF) is required for disassembly of the posttermination complex of the ribosome after release of polypeptides. The crystal structure of RRF resembles a tRNA shape, with an architecturally different flexibility compared with tRNA, but its structure-and-function relationships are unknown. We here found that an RRF variant defective in ribosome binding regains the binding capacity through 20 independent secondary changes occurring in three topologically distinct regions of RRF. Because two of these regions are equivalent to the tip of the anticodon stem and the upper surface of the acceptor stem of tRNA, RRF may interact with the ribosome in a way similar to tRNA, spanning 30S and 50S subunits, to exert its action for splitting the ribosome.

Keywords: intragenic suppressors; ribosome binding; ribosome recycling factor; RRF structure; tRNA mimic

INTRODUCTION

Translation termination proceeds in two sequential steps: The release of nascent polypeptides at stop codons and the disassembly of the posttermination complex (Ito et al., 2000). In bacteria, the ribosome recycling factor (RRF), in concert with the elongation factor EF-G, plays a main role in the second step for the next round of protein synthesis (for a review, see Janosi et al., 1996). After release of nascent polypeptides by polypeptide release factors RF1 and RF2, the ribosomal P-site and A-site remain occupied with a deacylated tRNA and RF1 or RF2 protein. Another class of bacterial release factor, RF3, accelerates the dissociation of RF1 and RF2 from the ribosome in a GTP-dependent manner, and RF3 is also released from the ribosome upon GTP hydrolysis (Freistroffer et al., 1997; Pavlov et al., 1997). These processes leave the posttermination complex with mRNA, deacylated tRNA in the P-site, and the empty A-site, which is believed to be a substrate for RRF in concert with EF-G (Hirashima & Kaji, 1972).

The crystal structure of RRF has recently been solved to 2.55, 2.3, and 2.6 Å resolution by three groups using RRF proteins from *Thermotoga maritima* (Selmer et al., 1999), *Escherichia coli* (Kim et al., 2000), and *Thermus thermophilus* (Toyoda et al., 2000). These three molecules are composed of two domains, domain 1 and domain 2, bridged by two loops (a hinge), and superimpose almost perfectly with $tRNA^{Phe}$ except for the amino acid-binding 3′ end. Selmer et al. (1999) have proposed that RRF is a near perfect tRNA mimic to explain the mechanistic disassembly of the posttermination ribosomal complex. They speculate that RRF binds to the A-site of the ribosome and that EF-G translocates RRF from the A- to the P-site and deacylated tRNA from the P- to the E-site of the ribosome in a GTP-dependent manner, where it would dissociate rapidly. RRF, however, is architecturally different from tRNA in that the hinge of RRF forms a flexible "gooseneck" elbow, whereas the elbow of tRNA is rigid, and this flexibility of RRF is vital for its function (Toyoda et al., 2000). Moreover, the model by Selmer et al. (1999) is not consistent with the biochemical findings of Karimi et al. (1999), which show, first, that RRF and EF-G split the ribosome into subunits in a reaction that requires GTP hydrolysis and, second, that the initiation factor IF3 is required for the removal of deacylated tRNA from the P-site of the 30S particle. Thus the mechanistic significance of a tRNA mimic by RRF remains to be tested. In fact, very little is known about the structure-and-function relationship of RRF, which piqued our interest in a functional mapping of the ribosome-binding site in RRF.

Reprint requests to: Yoshikazu Nakamura, Department of Basic Medical Sciences, The Institute of Medical Science, The University of Tokyo, P.O. Takanawa, Tokyo 108-8639, Japan; e-mail: nak@ims.u-tokyo.ac.jp.

RESULTS AND DISCUSSION

The rationale of functional mapping

The rationale of mapping the ribosome-binding site in this study was, first, to isolate a variant of *E. coli* RRF that is partially defective in the ribosome binding and, second, to select suppressor mutants that regain the activity to bind to the ribosome via secondary changes in the hope that these compensatory mutations will alter the site for the ribosome binding in a way that increases the binding capacity ("gain-of-function" phenotype). It is known that RRF is essential for bacterial growth (Janosi et al., 1998), and that the activity can be modulated by alteration in the C-terminal residues (Fujiwara et al., 1999). Accordingly, to screen for a reduced ribosome association form of RRF, we constructed a series of C-terminal deletions at two-amino-acid intervals in the RRF gene cloned in plasmid pIQV27 (renamed from pSUIQ; Uno et al., 1996) by nonsense substitutions (i.e., tandem UAA stop codons). These C-terminal truncations were examined for the complementation activity upon transformation of a temperature-sensitive RRF strain YN3576 (Fujiwara et al., 1999) or a RRF knockout strain (K. Ito and Y. Nakamura, unpubl.). One such deletion, ΔC9, lacking 9 amino acids, seemed to be appropriate as a parental form to select compensatory changes, given that its primary defect is in the ribosome binding, because the ΔC9 protein shows a temperature-sensitive phenotype, active at 30 °C but inactive at 42 °C in complementation (Fig. 1A), and a deletion mutant (in which tandem UAA stop codons substitute for the C-terminal 9 amino acids) would never revert to a wild-type form when suppressors are selected as survivors at 42 °C.

RRF variant defective in the ribosome binding

RRF is known to trigger a dissociation of the polysome complex into monosomes in vitro (Hirashima & Kaji, 1972). Hence, first, the ΔC9 and wild-type RRF proteins were overproduced and purified to homogeneity to test the protein activity in the conventional polysome breakdown assay. (We assume that the appearance of monosome fractions in the presence of RRF does not necessarily reflect the primary action mechanism of RRF because the assay uses crude polysome fractions under the condition that favors the reassembly of 30S and 50S subunits to 70S ribosomes.) The polysome fraction was prepared from exponentially growing *E. coli* cells (MRE600), incubated with wild-type and ΔC9 RRF proteins, and analyzed by sucrose density gradient centrifugation. As shown in Figure 2, wild-type RRF catalyzed polysome-to-monosome conversion, but the ΔC9 variant failed to do so. Next, we investigated whether or not the wild-type protein binds to the ribosome and, if so, if the ΔC9 protein binds to the ribosome as efficiently as does the wild type. The conventional sucrose density gradient analysis detects the fraction of [^{35}S]RRF associated with the 70S ribosome (Fig. 3A), showing that RRF forms a complex with the ribosome, but to a significantly lesser extent because translation factors are sensitive to the hydrostatic pressure generated by sucrose-gradient centrifugation (Celano et al., 1988). We therefore developed a reproducible (semi-) quantitative assay of precipitating [^{35}S]RRF–ribosome complexes loaded atop a 10% sucrose cushion using an ultracentrifuge (see Materials and Methods) according to the method described by Celano et al. (1988): Under this assay condition, the dissociation constant between wild-type RRF and the

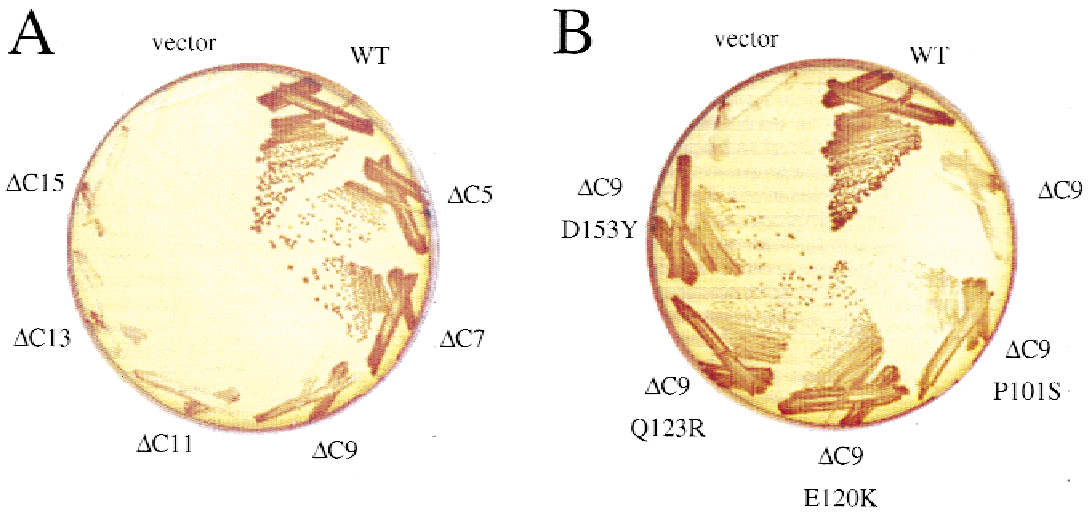

FIGURE 1. In vivo activity of RRF variants. **A**: Growth of YN3576 (carrying a high-temperature lethal RRF allele, *frr-3*) cells transformed with plasmid pIQV derivatives encoding C-terminally truncated RRF proteins at 42 °C. WT means wild-type RRF and C-terminal truncations at two-residue intervals are indicated as ΔC5 to ΔC15 where the number refers to the truncated amino acids. **B**: Growth restored by compensatory changes in the ΔC9 RRF. YN3576 transformants with pIQV-RRFΔC9 derivatives containing secondary changes were tested for growth at 42 °C.

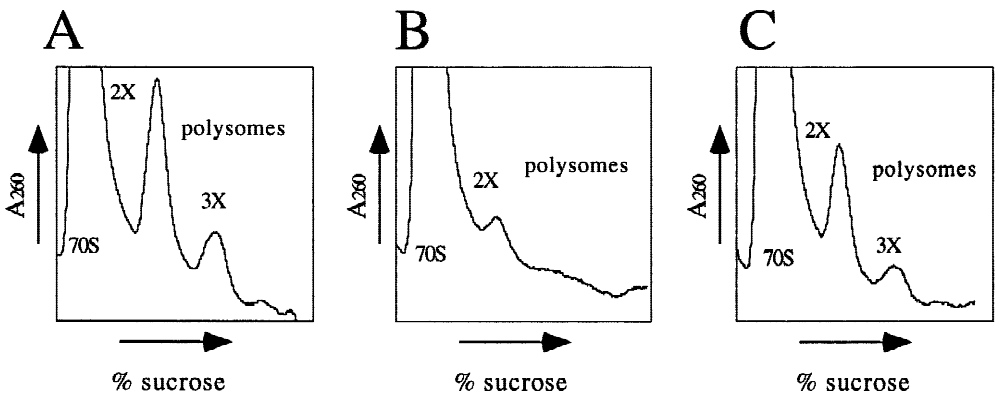

FIGURE 2. Polysome breakdown assay. 70S ribosomes were incubated in the absence of RRF (**A**) or in the presence of wild-type (**B**) and ΔC9 RRF (**C**) proteins, and analyzed by sucrose density gradient centrifugation.

ribosome was estimated to be around 0.4–0.7 μM (data not shown). In this assay, wild-type RRF efficiently competed with [^{35}S]RRF for binding to the ribosome, whereas ΔC9 protein competed only weakly (Fig. 3B). Therefore, the C-terminal deletion ΔC9 largely, if not completely, disables RRF binding to the ribosome, and the ΔC9 protein itself is stable in *E. coli* (data not shown). These protein features seem to fulfill the requirement for the parental strain, and primed us to select mutations compensatory for the ΔC9.

Gain-of-function in ribosome binding by compensatory changes

The RRFΔC9 DNA was mutagenized by error-prone polymerase chain reaction (PCR) or incubation with hydroxylamine in vitro (see Materials and Methods). The mixture of mutagenized DNAs was recloned to plasmid pIQV27 and transformed into a temperature-sensitive RRF strain YN3576, and transformants (Cm^R, chloramphenicol-resistant) were selected at 42 °C. Over

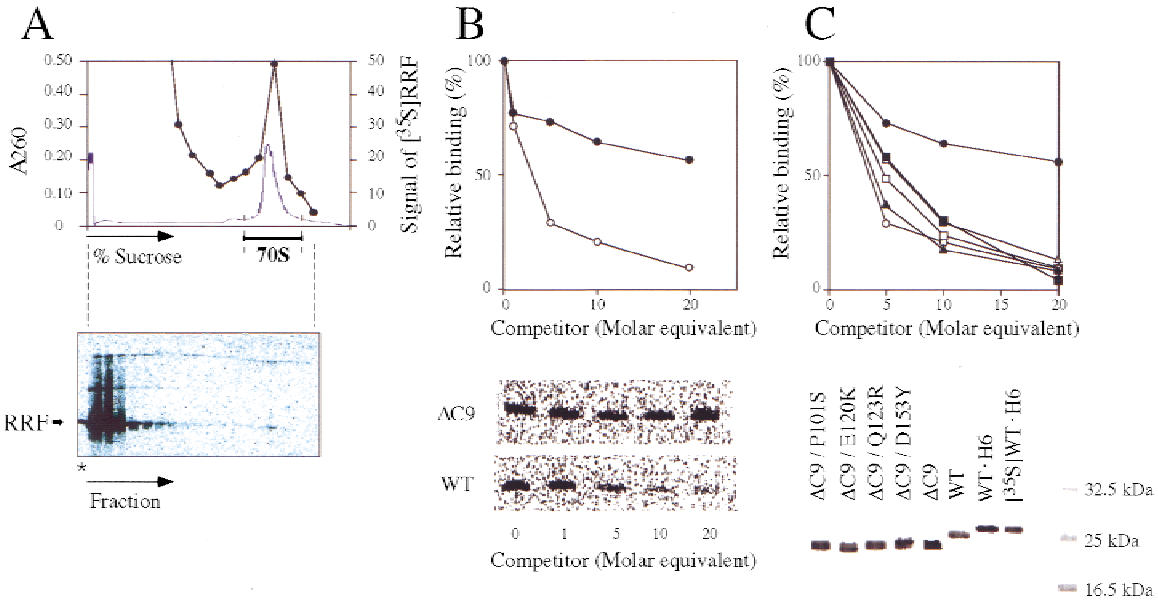

FIGURE 3. Binding between RRF variants and the ribosome. **A**: Association of [^{35}S]RRF with the 70S ribosome analyzed by sucrose density gradient centrifugation. Upper panel: fraction profile; lower panel, autoradioimage of [^{35}S]RRF. The asterisk indicates the control lane of [^{35}S]RRF. Each lane of both panels is shown at the same position. **B**: Binding competition with wild-type and ΔC9 RRF proteins. Experimental procedures are described in Materials and Methods. The intensity of [^{35}S]RRF bound to the ribosome in the presence of the indicated amounts (in fold molar excess relative to [^{35}S]RRF) of wild-type (open circles) and ΔC9 (closed circles) competitors (lower panel) was used to estimate the efficiency of competition as percentage of [^{35}S]RRF remaining in the ribosome precipitate (upper panel). **C**: Binding competition with ΔC9 RRF variants containing compensatory changes. Competitor proteins were purified to homogeneity as judged by Coomassie staining of proteins after SDS-polyacrylamide gel electrophoresis (lower panel), and challenged to the [^{35}S]RRF–ribosome interaction. Symbols: open circles, wild-type RRF; closed circles, ΔC9 RRF; open squares, ΔC9•D153Y RRF; closed squares, ΔC9•Q123R RRF; open triangles, ΔC9•E120K RRF; closed triangles, ΔC9•P101S RRF.

100 survivors were characterized by DNA sequencing, and 45 independent plasmid clones bearing single substitutions were isolated and shown to restore the growth of not only YN3576 but also a knockout RRF strain at 42 °C (Fig. 1B). By DNA sequencing, ΔC9-suppressor mutations were classified as one of 20 single amino acid substitutions occurring at 15 positions with a broad range of suppression efficiency (Table 1). Because identical substitutions were repeatedly found in different isolates, the selection was nearly saturated, suggesting that we are probably dealing with most, if not all, of the available alterations.

Positions of 15 amino acids showing the suppressor function were classified into three distinct areas of the tertiary structure of RRF (Fig. 4): eight at or near the tip of domain 1 (class I), four at the upper surface of domain 2 (class II), and four at the upper part of domain 1 (class III). Given a tRNA mimic, class I and class II sites are topologically equivalent to the tip of the anticodon stem and the upper surface of the acceptor stem of tRNA, respectively. Because anticodon stem and the acceptor stem of tRNA interact with the decoding site of 16S rRNA and the peptidyltransferase site of 23S rRNA, respectively, mimicry would imply that class I residues interact with 30S ribosomes and class II residues interact with 50S ribosomes. The class III residues are close to ΔC9 in the tertiary structure. Although the reason for the ribosome-binding defect in ΔC9 is not known, we assume that class III alterations may restore the functional conformation at or near the ΔC9.

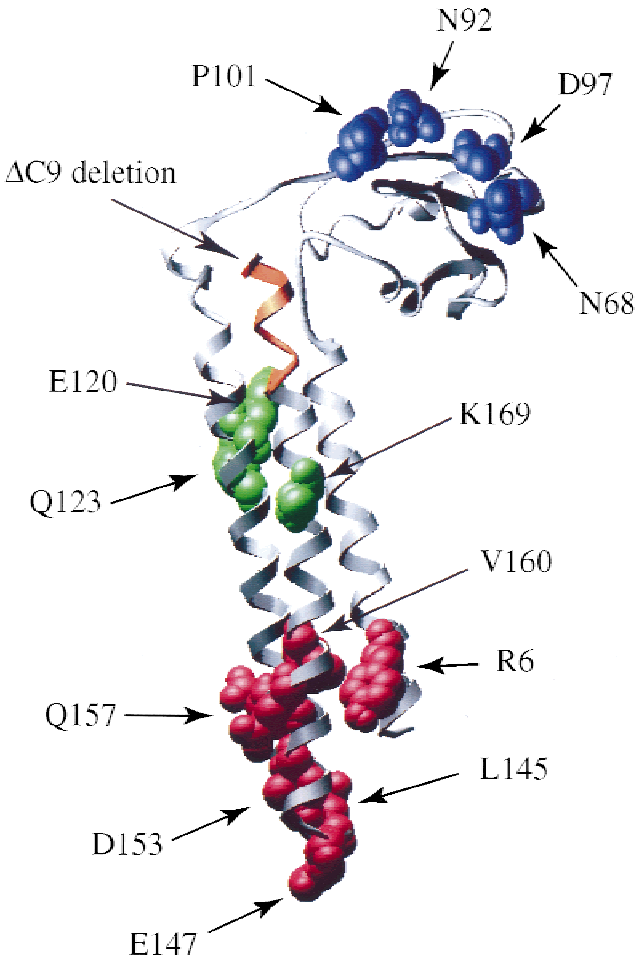

FIGURE 4. Structural distribution of amino acid changes showing gain of function in binding to the ribosome. Class I, II and III residues are colored red, blue and green, respectively, in the ribbon diagram of RRF (Protein Data Bank accession code 1EH1) showing the overall fold. The C-terminal 9 amino acids are colored orange.

TABLE 1. Gain-of-function alterations for ribosome binding.

Substitutions	Classification	Number of isolates	Suppression activity[a]
Arg6 → Ile	class I	3	++
Asn68 → Ser	class II	1	+
Asn92 → Ile	class II	1	++
Asn92 → Tyr	class II	2	+
Asp97 → Val	class II	1	+
Pro101 → Leu	class II	1	+
Pro101 → Ser	class II	1	+
Glu120 → Lys	class III	1	+
Gln123 → Arg	class III	3	++
Asp137 → Asn	class I	1	+
Leu143 → Ser	class I	1	+
Asp145 → Asn	class I	1	+
Glu147 → Lys	class I	1	++
Asp153 → Gly	class I	13	++
Asp153 → Asn	class I	1	+
Asp153 → Val	class I	2	+++
Asp153 → Tyr	class I	3	+++
Gln157 → Arg	class I	4	++
Val160 → Ile	class I	3	++
Lys169 → Asn	class III	1	+

[a]Monitored by growth at 42 °C of YN3576 cells transformed with pIQV-RRFΔC9 variants carrying the indicated substitutions. Suppression activity was scored by colony size and growth: +++: normal growth (large colony); ++: fair growth (medium colony); +: weak growth (small colony).

For the ribosome-binding assay, we purified four mutant proteins that respectively contain P101S, E120K, Q123R, and D153Y substitutions plus ΔC9; together, these proteins represent all three classes. All these doubly altered proteins acquired the capacity to compete with [^{35}S]RRF for efficient binding to the ribosome, or only slightly less than efficient binding, as in the case of wild-type RRF (Fig. 3C). Therefore, these secondary changes compensate for the ΔC9-induced ribosome entry defect by directly activating the ribosome-binding site(s) or indirectly restoring the functional conformation of the ΔC9 site.

Implications for a tRNA mimic

Crystallographic studies of three bacterial RRF proteins have shown that RRF is a tRNA-like L-shaped molecule

consisting of two domains (see Fig. 4): a long three-helix bundle (domain 1) and a three-layer $\beta/\alpha/\beta$ sandwich (domain 2) (Selmer et al., 1999; Kim et al., 2000; Toyoda et al., 2000). These two domains are bridged by two loops that function as a flexible hinge. Although the individual domain structures are similar, the interdomain angle is potentially variable and the hinge flexibility is vital for the function of RRF (Toyoda et al., 2000). The hinge flexibility can be modulated by altering amino acids in the hinge or the region in direct contact with the hinge, including the C terminus of RRF. Because a hinge structure that is too relaxed is unable to function (Toyoda et al., 2000), we assume that the truncation of the C-terminal 9 amino acids (see orange region in Fig. 4) may impair the active conformation of the hinge and/or the three-helix bundle in domain 1, so that RRF no longer binds to the ribosome. Three residues assigned as class III alterations are located spatially close to the ΔC9 truncation; these are charge-flip changes (Table 1). Therefore, one might speculate that the increased electrostatic attraction within this microenvironment may play a role in stabilizing the three-helix bundle structure or the functional hinge conformation, although other explanations might also be possible. Consistently, the ΔC9 protein is less stable in vivo than the wild type, and this instability is corrected by class III changes (data not shown).

From the standpoint of the tRNA mimic, it is reasonable to speculate that class I amino acids correspond to nucleotides at or near the tip of the anticodon stem of tRNA and directly interact with the decoding site of the 30S ribosome. All 11 class-I substitutions occurring at the eight positions are charge-flip changes of decreasing negative charges or increasing positive charges, with the exception of two substitutions for Leu143 and Val160 (Table 1). Therefore, these changes are likely to increase electrostatic attraction with the negatively charged phosphate backbone of 16S rRNA or ribosomal protein(s), if any. Since the A-site must be very carefully designed to hold tRNA and mRNA in sterically well-defined positions of 16S rRNA (Yoshizawa et al., 1999), RRF may mimic, at least in part, the mode of tRNA docking to the ribosome. In contrast to class I alterations, class II residues are localized on the surface of domain 2 that is equivalent to the acceptor stem of tRNA. Of the six class-II substitutions occurring at four positions, most are hydrophobic changes not associated with a charge flip, with the exception of the substitution for Asp97. The amino acid-binding 3′ (CCA) end of the acceptor stem of tRNA is held in sterically well-defined positions of 23S rRNA (Cate et al., 1999). RRF misses a structural counterpart of CCA. Hence it remains to be clarified what part of the 50S ribosome, 23S rRNA or large ribosomal protein(s), interacts with the class-II residues of RRF.

The majority (33/45) of isolates showing gain of function in binding to the ribosome are clustered on the tip of domain 1, and these alterations frequently produce a strong phenotype of compensating for the growth defect by ΔC9 (Table 1). Asp153 is quite a hot spot: About half of the isolates (19/45) changed Asp153 to four different amino acids, two of which, D153V and D153Y, are phenotypically the strongest suppressors equivalent to the wild type. This suggests that Asp153 is placed at the interface between domain 1 of RRF and the ribosome, and may directly or indirectly strengthen the capacity of RRF to bind to the ribosome, perhaps to the phosphate chain of 16S rRNA, upon removal of its negative charge. In parallel to the experiment described here, we also carried out the selection of compensatory changes for the ΔC11 variant exerting a more severe defect than ΔC9. Only one survivor has thus far been isolated, and it turned out to possess double mutations, D153Y (class I) and Q123R (class III). Either allele alone did not efficiently restore the defect of ΔC11, indicating that two strong alterations in distinct sites are necessary to compensate for such a severe defect as ΔC11.

It is noteworthy that the 15 affected positions in suppressor mutants—all those but Val160—are nonconservative residues. If most, or all, of these amino acids are involved in the ribosome binding, their interaction sites may also be diverse in amino acid or nucleotide species. Alternatively, the most crucial residues for the ribosome binding may be conservative, and their binding capacity may be enhanced indirectly by alterations in nonconservative neighboring residues.

CONCLUSION

The present findings suggest that RRF interacts with the ribosome in a way similar to tRNA, spanning 30S and 50S subunits, for exerting its action using the flexible gooseneck, and that the ΔC9 is likely to diminish this action by affecting the hinge structure. If RRF binds to the A-site of the ribosome in a manner similar to tRNA and splits the ribosome into subunits, RRF must exert its action within the A-site in concert with EF-G. EF-G can generate a post- to pre-peptidyl-transfer transition state of the ribosome coupled with GTP hydrolysis. This energy-driven transition may involve distortion of the interface between 30S and 50S ribosome particles. Therefore, it is tempting to speculate that either of the domains connected by the flexible gooseneck of RRF may penetrate into a distorted interface and interfere with post- to pre-peptidyl-transfer transition, shifting the equilibrium toward a direct uncoupling of 30S and 50S.

MATERIALS AND METHODS

Protein overexpression and purification

E. coli BL21(DE3) transformed with pET30a (Novagen, Inc.) derivatives encoding wild-type and mutant RRF proteins without a histidine tag was grown in LB medium (1 L) at 37 °C

(wild-type) or 16 °C (ΔC9 and its derivatives) to the cell density of 0.6 A_{600}. Expression of RRF was induced by addition of isopropyl-1-thio-β-D-galactoside (IPTG, final 1 mM), followed by 2 h culture at 37 °C. Harvested cell paste was suspended in buffer A (50 mM Tris-HCl, pH 7.0, 10 mM $MgCl_2$, 5 mM dithiothreitol) containing 0.5 M NH_4Cl, and sonicated. The cell debris and ribosomes were removed from the cell lysate by two successive centrifugations (12,000 × *g* for 20 min and 150,000 × *g* for 2 h). Crystalline ammonium sulfate was added to the cleared supernatant up to 50% saturation. Protein precipitates were dialyzed against buffer B (10 mM Tris-HCl, pH 7.8, 50 mM KCl, 1 mM dithiothreitol), and passed through a DEAE-Sephadex A50 column equilibrated with buffer B. The flow-through fraction was dialyzed against buffer C (10 mM Tris-HCl, pH 6.5, 5 mM KCl, 1 mM dithiothreitol) and subjected to ÄKTA RESOURCE S (Pharmacia) column chromatography using a linear gradient of 5–150 mM KCl. Wild-type RRF eluates with 40 mM KCl, whereas the ΔC9 protein and its derivatives are recovered in the flow-through fraction. RRF proteins were further concentrated, if necessary, using a Centriplus YM-10 ultrafiltration (Millipore) to yield 5–80 mg of pure proteins. To prepare [^{35}S]RRF protein, the wild-type RRF sequence was cloned into the *Nde*I-*Sal*I sites of plasmid pET30a, and the histidine-tagged RRF protein was expressed essentially as described above except that cells were grown in minimal medium E (Miller, 1972) (100 mL) in the presence of redivue Pro-mix L-[^{35}S] in vitro cell labeling mix (1 mCi, Amersham Pharmacia Biotech). Cells were lysed using BugBuster™ Protein Extraction Reagent and Kits (Novagen), and the histidine-tagged [^{35}S]RRF protein (2 mg) was purified to homogeneity from cell lysates by affinity chromatography using ProBond™ Resin (Novagen) according to the manufacturer's instructions.

Plasmids and manipulations

Plasmid pIQV-RRF is an IPTG-controllable RRF expression plasmid that encodes the *E. coli* RRF gene at the *Xba*I-*Sal*I sites of pIQV27. A series of C-terminal deletions were created by PCR amplification using M13 reverse primer (5′-TGTGGAATTGTGAGCGG-3′) and RRF sense primers containing UAA stop codons at two amino acids intervals:

ΔC5: 5′-CCCCGTCGACTTATTATGCTTCTTTGTCTGCCAGCGC-3′;
ΔC7: 5′-CCCCGTCGACTTATTATTTGTCTGCCAGCGCCGCTTC-3′;
ΔC9: 5′-CCCCGTCGACTTATTATGCCAGCGCCGCTTCAATTTTC-3′;
ΔC11: 5′-CCCCGTCGACTTATTACGCCGCTTCAATTTTCTTGATTGC-3′;
ΔC13: 5′-CCCCGTCGACTTATTATTCAATTTTCTTGATTGCAGC-3′; and
ΔC15: 5′-CCCCGTCGACTTATTATTTCTTGATTGCAGCATCAGTC-3′.

Wild-type, ΔC9, and suppressor mutant sequences were recloned from pTWV228 derivatives into the *Xba*I-*Sal*I site of plasmid pET30a. DNA manipulations were conducted according to standard methods (Sambrook et al., 1989).

Mutant selection

The RRFΔC9 sequence cloned in plasmid pTWV228 (TaKaRa Co.) was mutagenized with 0.4 M hydroxylamine as described previously (Oshima et al., 1995) or by error-prone PCR amplification using M13 primers M4 and RV according to the standard procedures (Beckman et al., 1985). These DNAs were trimmed with *Xba*I and *Sal*I, inserted into plasmid pIQV27, and transformed into a high-temperature lethal *frr-3* strain YN3576. Cm^R transformant survivors were selected at 42 °C on LB agar medium (Miller, 1972) and plasmid DNAs that gave a reproducible phenotype upon retransformation were further characterized. The entire coding part of RRF was amplified from these suppressor variants by PCR and analyzed by DNA sequencing and complementation.

Ribosome binding assay

NH_4Cl-washed ribosomes (1 M) were prepared from MRE600 (Cammack & Wade, 1965) cells according to the procedures described previously (Pestka, 1968). The resulting 70S ribosome (30 pmol) was mixed with [^{35}S]RRF (10 pmol) in the presence or absence of the indicated amounts of competitor variants in 50 μL binding solution (10 mM Tris-HCl, pH 7.6, 100 mM NH_4Cl, 10 mM $MgSO_4$, 1 mM dithiothreitol, 5 μg bovine serum albumin). The binding mixture was incubated at 33 °C for 10 min, quickly loaded onto an ice-cold 10% sucrose cushion (50 μL), and centrifuged at 95,000 rpm for 30 min using a Hitachi CS120EX Ultracentrifuge at 4 °C. The precipitated ribosomal complex was analyzed by SDS-polyacrylamide gel electrophoresis, and the intensity of ^{35}S-labeled band was measured using a BioImage analyzing system 2000 (Fuji Film, Tokyo).

Polysome breakdown assay

Polysome was prepared from strain MRE600 essentially as described previously (Hirashima & Kaji, 1972). Briefly, exponentially growing cells were lysed, and the lysate was subjected to Sepharose 6B column chromatography. The polysome fraction as judged by the sucrose density gradient centrifugation was incubated with RRF under the conditions described previously (Hirashima & Kaji, 1972), and analyzed by 15–30% sucrose density gradient centrifugation.

ACKNOWLEDGMENTS

This work was supported in part by grants from The Ministry of Education, Science, Sports and Culture of Japan (to Y.N.); the Human Frontier Science Program (awarded in 1993 and 1997 to Y.N.); and the BRAIN Basic Research for Innovation Biosciences Program of Bio-oriented Technology Research Advancement Institution, Japan (to Y.N). K.I. is a BRAIN Research Fellow.

Received August 23, 2000; returned for revision September 21, 2000; revised manuscript received October 11, 2000

REFERENCES

Beckman RA, Mildvan AS, Loeb LA. 1985. On the fidelity of DNA replication: Manganese mutagenesis in vitro. *Biochemistry 24*: 5810–5817.

Cammack KA, Wade HE. 1965. The sedimentation behavior of ribonuclease-active and -inactive ribosomes from bacteria. *Biochem J 96*:671–680.

Cate JH, Yusupov MM, Yusupova GZ, Earnest TN, Noller HF. 1999. X-ray crystal structures of 70S ribosome functional complexes. *Science 285*:2095–2104.

Celano B, Pawlik RT, Gualerzi CO. 1988. Interaction of *Escherichia coli* translation-initiation factor IF-1 with ribosomes. *Eur J Biochem 178*:351–355.

Freistroffer DV, Pavlov MY, MacDougall J, Buckingham RH, Ehrenberg M. 1997. Release factor RF3 in *E. coli* accelerates the dissociation of release factors RF1 and RF2 from the ribosome in a GTP-dependent manner. *EMBO J 16*:4126–4133.

Fujiwara T, Ito K, Nakayashiki T, Nakamura Y. 1999. Amber mutations in ribosome recycling factors of *Escherichia coli* and *Thermus thermophilus*: Evidence for C-terminal modulator element. *FEBS Lett 447*:297–302.

Hirashima A, Kaji A. 1972. Factor-dependent release of ribosomes from messenger RNA: Requirement for two heat-stable factors. *J Mol Biol 65*:43–58.

Ito K, Uno M, Nakamura Y. 2000. A tripeptide 'anticodon' deciphers stop codons in messenger RNA. *Nature 403*:680–684.

Janosi L, Hara H, Zhang S, Kaji A. 1996. Ribosome recycling by ribosome recycling factor (RRF)—an important but overlooked step of protein biosynthesis. *Adv Biophys 32*:121–201.

Janosi L, Mottagui-Tabar S, Isaksson LA, Sekine Y, Ohtsubo E, Zhang S, Goon S, Nelken S, Shuda M, Kaji A. 1998. Evidence for in vivo ribosome recycling, the fourth step in protein biosynthesis. *EMBO J 17*:1141–1151.

Karimi R, Pavlov M, Buckingham R, Ehrenberg M. 1999. Novel roles for classical factors at the interface between translation termination and initiation. *Mol Cell 3*:601–609.

Kim KK, Min K, Suh SW. 2000. Crystal structure of the ribosome recycling factor from *Escherichia coli*. *EMBO J 19*:2362–2370.

Miller J. 1972. *Experiments in molecular genetics*. Cold Spring Harbor, New York: Cold Spring Harbor Laboratory Press.

Oshima T, Ito K, Kabayama H, Nakamura Y. 1995. Regulation of *lrp* gene expression by H-NS and Lrp proteins in *Escherichia coli*: Dominant negative mutations in *lrp*. *Mol Gen Genet 247*:521–528.

Pavlov MY, Freistroffer DV, MacDougall J, Buckingham RH, Ehrenberg M. 1997. Fast recycling of *Escherichia coli* ribosomes requires both ribosome recycling factor (RRF) and release factor RF3. *EMBO J 16*:4134–4141.

Pestka S. 1968. Studies on the formation of transfer ribonucleic acid-ribosome complexes. 3. The formation of peptide bonds by ribosomes in the absence of supernatant enzymes. *J Biol Chem 243*:2810–2820.

Sambrook J, Fritsch EF, Maniatis T. 1989. *Molecular cloning: A laboratory manual*, 2nd ed. Cold Spring Harbor, New York: Cold Spring Harbor Laboratory Press.

Selmer M, Al-Karadaghi S, Hirokawa G, Kaji A, Liljas A. 1999. Crystal structure of *Thermotoga maritima* ribosome recycling factor: A tRNA mimic. *Science 286*:2349–2352.

Toyoda T, Tin OF, Ito K, Fujiwara T, Kumasaka T, Yamamoto M, Garber MB, Nakamura Y. 2000. Crystal structure combined with genetic analysis of the *Thermus thermophilus* ribosome recycling factor shows that a flexible hinge may act as a functional switch. *RNA 6*:1432–1444.

Uno M, Ito K, Nakamura Y. 1996. Functional specificity of amino acid at position 246 in the tRNA mimicry domain of bacterial release factor 2. *Biochimie 78*:935–943.

Yoshizawa S, Fourmy D, Puglisi JD. 1999. Recognition of the codon–anticodon helix by ribosomal RNA. *Science 285*:1722–1725.